

TiAl₃ formation by furnace annealing of Ti/Al bilayers and the effect of impurities

X.-A. Zhao,^{a)} F. C. T. So,^{b)} and M.-A. Nicolet
California Institute of Technology, Pasadena, California 91125

(Received 31 August 1987; accepted for publication 8 December 1987)

Reactions of Ti/Al couples induced by furnace annealing were investigated (at elevated temperature) using large-grained Al substrates and vacuum-evaporated bilayers of both sequences. ⁴He MeV backscattering spectrometry was principally used to monitor the reactions. Profiles of oxygen impurity were obtained by elastic ¹⁶O(α,α')¹⁶O resonant scattering. In the range of 460–515 °C, TiAl₃ forms as a laterally uniform layer at the Ti/Al interface. The thickness of this compound layer increases as (annealing time)^{1/2}. The activation energy is 1.9–2.0 ± 0.1 eV. For evaporated bilayers on an oxidized Si substrate, the sequence of the bilayers does not effect the growth mechanism of TiAl₃, but the growth rate of samples with the Ti on top is lower than that of samples with Al on top, that is, oxygen in Ti/Al samples can reduce the reaction rate by decreasing the pre-exponential factor. Oxygen already contained in the Ti film and oxygen from the annealing ambient are incorporated in the growing TiAl₃ compound during thermal annealing. In addition, a TiAl₃ layer also forms at the free Ti surface during vacuum annealing when the oxygen-containing contaminants in the ambient are minimized. So far, we succeeded in accomplishing this only for large-grained Al substrates. We conclude that the formation of the TiAl₃ compound at the surface is controlled by nucleation and depends sensitively on the condition of the surface layer of the Ti film.

I. INTRODUCTION

Ti and its alloys have attracted recent attention as barrier layers to separate Al from Si in very large scale integration metallizations.^{1,2} The Al/Ti system has been studied in detail before.^{3–11} When adjoining Al and Ti thin films react, the intermetallic compound TiAl₃ forms. The compound grows according to diffusion-controlled kinetics. Activation energies varying from 1.6 to 1.85 eV were obtained by different researchers. Aluminum is a dominant moving species as was determined by inert marker experiment.^{9,12} Moreover, it has also been found by transmission electron microscopy⁸ that in polycrystalline bilayers TiAl₃ forms as a continuous film that penetrates deeply into the Al grain boundaries. This observation proves that Ti can also be the predominant moving species. In contrast, the growth of TiAl₃ in the presence of 1% Cu solute in Al is independent of the Al grain boundaries. As a result, the latter TiAl₃/Al interface is much smoother than the former. In addition, the grain size of the Al layer is larger with added Cu than without. Therefore, it is of interest to know how the reaction proceeds when single-crystalline (Al) is used instead of a polycrystalline Al thin film. We partly answer this question in the present paper.

In our previous study of the Ni/Al system,¹³ we have shown that the use of Al substrates with large crystalline grains (a few millimeters and up to 1 cm in diameter) avoids the severe diffusion of Ni atoms along the Al grain boundaries and results in a uniform growth of NiAl₃ with reproduc-

ible kinetics. These facts allow one to investigate the growth kinetics of aluminide reliably and conveniently by backscattering spectrometry and they also provide opportunities to compare the formation processes of aluminides with those of silicides. The latter have been well characterized for the corresponding configuration of a transition-metal film on a Si single-crystalline substrate.

We investigate here the initial aluminide phase formed during the thermal reaction of polycrystalline Ti on large-grained Al substrates induced by furnace annealing. Experiments with polycrystalline thin-film couples of Ti/Al have also been carried out for a comparison. The range of annealing temperatures investigated here is 460–515 °C, which is closer to the common processing temperatures than that of previous studies (375–450 °C).

It is known from metal/Si investigations that impurities can affect the kinetics and the nucleation and the growth of interfacial compounds.^{14,15} Oxygen contamination has a foremost influence, both as a contaminant in films and as an oxide layer at the interface and in grain boundaries. The far reaching effect of undetected impurities is surely the cause of many of the observed inconsistencies in thin-film reactions reported in the literature. In the particular case of Ti, the oxygen concentration in the film strongly depends on the deposition condition. In addition, oxygen is absorbed in the film and a surface oxide forms quickly when a Ti film is exposed to air. Subsequent annealing, even in a good vacuum, typically increases and redistributes the oxygen because Ti is highly reactive with oxygen.^{16,17} Hence, it is essential in working with Ti to assess the role of oxygen by measuring its presence and monitoring its behavior during a reaction. In this work, the elastic resonant scattering of 3.05-MeV ⁴He⁺ by ¹⁶O was employed to probe the oxygen distribu-

^{a)} Permanent address: Shanghai Institute of Metallurgy, Academy of Sciences of China, Shanghai, China.

^{b)} Present address: Optoelectronics Division, Hewlett-Packard Company, San Jose, CA 95131.

tion.¹⁸ The nondestructive character of this reaction allows oxygen profiling without interference by adventitious oxygen during the measurement.

II. EXPERIMENTAL PROCEDURES

Large-grained Al substrates (" $\langle\langle\text{Al}\rangle\rangle$ ") were prepared from commercial high-purity (99.999%) Al plates about 1 mm thick. The method applied here uses many cold rolling and annealing cycles. This strain annealing technique is described in Ref. 19. The cycle is repeated until a satisfactory grain size is attained as determined visually after etching the processed plate in a warm NaOH solution. These substrates were chemically cleaned before loading into an oil-free evaporation system. A Ti layer of about 2000–3500 Å was *e*-gun deposited onto the substrates, preceded immediately by an argon dc sputter-cleaning cycle. The vacuum during deposition at a rate of 15 Å/s was better than 3×10^{-7} Torr. Details on the Al grain growth and sputter-cleaning processes can be found in Ref. 13. Thin-film bilayer samples were also prepared by sequentially *e*-gun depositing Al (~ 4000 Å) and Ti (~ 2000 Å), or in reverse order, on oxidized Si wafers. The conditions for these Ti evaporations equaled those of above; the pressure during Al evaporation was about 2×10^{-7} Torr.

Thermal treatment was carried out in an oil-pumped and liquid-nitrogen-trapped vacuum furnace that reaches about 7×10^{-7} Torr. To assure a valid comparison of reaction kinetics, both large-grained and thin-film samples were simultaneously annealed for varying temperatures and durations. To observe the effects of annealing ambient on the reactions, some of the thin-film samples were treated under different annealing conditions as will be described below.

The thickness and composition of various aluminide layers formed were measured by 1.8- and 3.0-MeV He backscattering spectrometry and their compounds were confirmed by glancing angle x-ray diffraction. The oxygen profiles in samples before and after aluminide formation were quantitatively determined with the scanning oxygen-resonance technique by using as the calibration standard a thick SiO₂ sample where the oxygen density was taken to be 4.6×10^{22} atom/cm³, absolutely.

III. RESULTS

A. Annealing procedure (vacuum, without protection)

When conventional procedures were used to anneal Ti/Al couples, with Ti on top, that is, the vacuum system was only evacuated to a base pressure of about 7×10^{-7} Torr without any preannealing of the system before starting to heat treat the samples, the reactions stalled after only half of the deposited Ti film was consumed, whatever the temperature was (from 460 to 515 °C). We also noted a residual gas evolution in the first few minutes after sliding the moveable boat with the sample into the center of the furnace. At that time, the vacuum pressure rose to $3\text{--}6 \times 10^{-6}$ Torr. The conventional procedures were therefore improved as follows (referred to as annealing procedure I): The quartz tube system was pumped down to the base pressure and then each

boat was pushed into the center of the furnace and baked for 20 min, one after another, at a temperature which was 100 °C above the highest annealing temperature subsequently used. The system was then vented with dry nitrogen that kept flowing during the loading of samples into their boats. The loading and reevacuation were done as quickly as possible. With this improved procedure, the whole Ti films could be transformed laterally uniformly to a compound layer.

Typical backscattering spectra showing the growth of TiAl₃ obtained at 462 °C according to this annealing procedure for Al/Ti/SiO₂/ $\langle\langle\text{Si}\rangle\rangle$, Ti/ $\langle\langle\text{Al}\rangle\rangle$, and Ti/Al/SiO₂/ $\langle\langle\text{Si}\rangle\rangle$ are presented in Figs. 1, 2(a), and 2(b) respectively. It is readily seen that in all cases a well-defined aluminide phase grows uniformly at the Ti/Al interface. The relative composition of the aluminide layer can be determined from the heights of the Al and Ti signals, as shown in Figs. 1 and 2. The atomic ratio of Ti to Al, calculated in the surface energy approximation,²⁰ is $1:3 \pm 15\%$, indicative of the formation of the compound TiAl₃. This phase is also the only one detectable by glancing angle x-ray diffraction over the temperature range investigated here. These results agree with earlier work.^{4–10} Notice that the spectra of Figs. 1 and 2(a) indicate smooth planar interfaces. There is no initial diffusion of Ti into the polycrystalline Al along grain boundaries, as has been reported recently for Al/Ti⁹ and as was also seen for evaporated Pt/Al couples.²¹

We have measured the amount of TiAl₃ that grows as a function of time for several annealing temperatures. In Fig. 3, the squares of the amounts of TiAl₃ formed are plotted against the annealing duration for all three types of samples. In all three cases each set of data points for different temperatures can be least-squares fitted to a straight line characteristic of a diffusion-limited process for the phase growth. All these lines, when extended, pass near the origin. This fact implies that there is little incubation time, as is typically observed when interfacial impurity layers are present, and that little TiAl₃ exists prior to annealing.

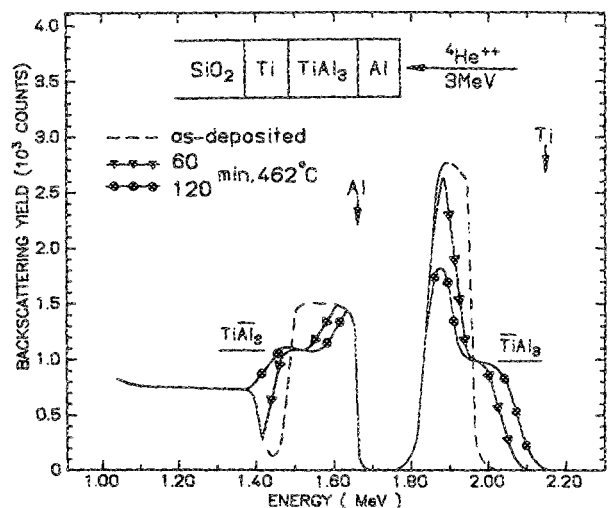


FIG. 1. 3.0 MeV $^4\text{He}^+$ backscattering spectra of vacuum-evaporated bilayer of 4580-Å Al on 1660-Å Ti on SiO₂ before (dashed line) and after 462 °C annealing for 60 min (triangles) and for 120 min (circles). The beam incidence is normal to the surface of the sample. The detector is at 170° with respect to the incident beam; this detector position applies for all backscattering spectra in this paper.

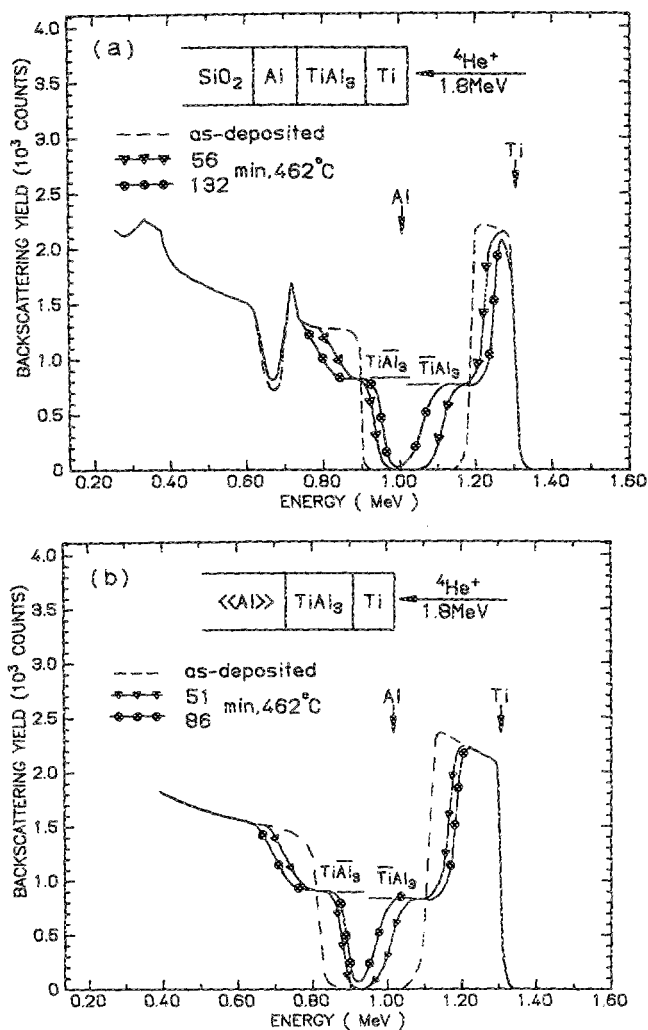


FIG. 2. 1.8 MeV $^4\text{He}^+$ backscattering spectra: (a) evaporated films of 1860-Å Ti on 3410-Å Al on a SiO_2 substrate before (dashed line) and after 462 °C annealing for 56 min (triangles) and for 132 min (circles); (b) 2320 Å on large-grained Al substrate before (dashed) and after 462 °C annealing for 51 min (triangles) and 86 min (circles).

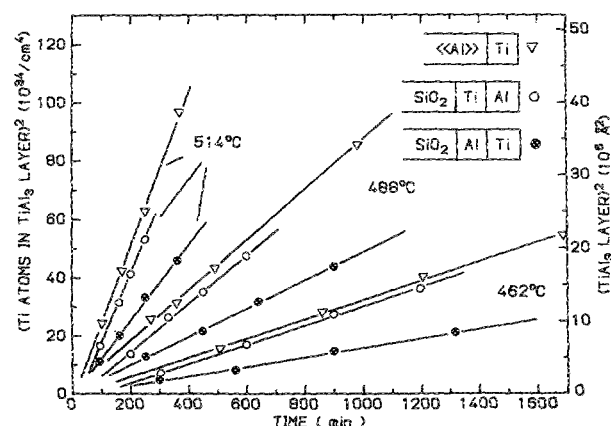


FIG. 3. The square of the amount of TiAl_3 formed vs annealing duration for $\text{Ti}/\langle\text{Al}\rangle$ (triangles), and $\text{Al}/\text{Ti}/\text{SiO}_2$ (open circles), and $\text{Ti}/\text{Al}/\text{SiO}_2$ (full circles). The vertical axis is calibrated in Ti atoms/ cm^2 contained in the TiAl_3 layer. This scale can be converted (approximately) to actual thickness by dividing the number of Ti atoms/ cm^2 through the density of a formula unit of TiAl_3 , i.e., $1.57 \times 10^{22}/\text{cm}^3$,²² as shown on the right-hand side (annealing procedure 1).

ent, and that little TiAl_3 exists prior to annealing.

However, the rate of growth is not the same for all samples. The growth rates for the $\text{Al}/\text{Ti}/\text{SiO}_2/\langle\text{Si}\rangle$ and $\text{Ti}/\langle\text{Al}\rangle$ samples are close, but that for the $\text{Ti}/\text{Al}/\text{SiO}_2/\langle\text{Si}\rangle$ is about $2^{-1/2}$ slower. In terms of sensitivity of a sample to adventitious impurities picked up from its surroundings, we may consider $\text{Al}/\text{Ti}/\text{SiO}_2/\langle\text{Si}\rangle$ samples to be the most immune and a reference case, because the native surface oxide of Al protects the sample from further oxidation in the annealing ambient or in air. We support this contention below. It then seems odd that the growth rates obtained for the two sample configurations where Ti is exposed to air in transport and subsequently to vacuum during annealing should be as dissimilar as they are. It is even more surprising that the exposed Ti film on large-grained Al reacts slightly faster than that of the reference sample. One fact which can explain the observation is that the large-grained Al substrate certainly is purer (nominally 99.999% as acquired) than the evaporated Al films. Since Al is also the dominant moving species in this reaction, the impurities in the Al can also effect the formation of TiAl_3 .¹⁴

Arrhenius plots of the growth constants, K (defined by $x^2 = Kt$, where x is the thickness of the TiAl_3 layer and t is the annealing duration), deduced from Fig. 3 are reported in Fig. 4. The plots yield the activation energies and the pre-exponential factors, which are listed in Table I, after a negligible incubation period. The activation energy for all sample configurations are the same within our experimental error of ± 0.1 eV. We conclude that oxygen content affects the reaction rate but not the mechanism responsible for the Al diffusion in the TiAl_3 layer, for which an argument is given in the discussion section.

B. Annealing procedure 2 (forming gas)

To observe the effect of the annealing ambient on the reaction, the two samples with different sequences of evapo-

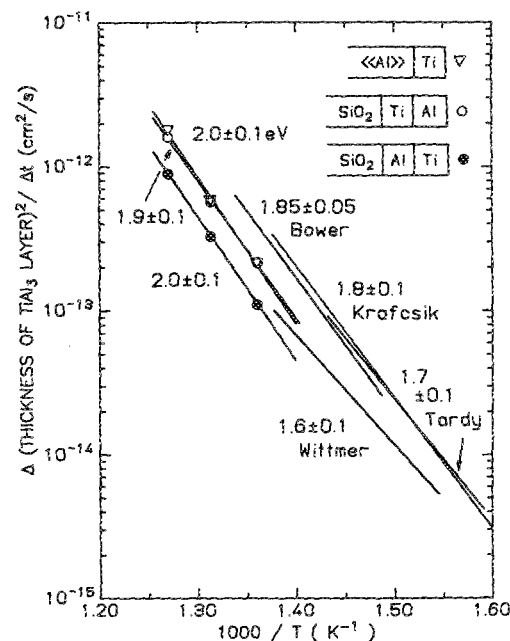


FIG. 4. Arrhenius plots obtained from the TiAl_3 growth rates shown in Fig. 3. Data obtained from the literature are included for comparison.

TABLE I. Pre-exponential factor K_0 and activation energy E_a of the growth constant K of $TiAl_3$.

Sample of configuration	Reference No.	K_0 (cm^2/s)	E_a (eV)	Annealing temp. range ($^{\circ}C$)
Al/Ti/SiO ₂ / \langle Si	9	2.4×10^{-1}	1.72 ± 0.10	350-425
Al/Ti/SiO ₂ / \langle Si	8	1.4×10^{-2}	1.6 ± 0.1	375-450
Al/Ti/SiO ₂ / \langle Si	6	0.2	1.8 ± 0.1	350-450
Al/Ti/SiO ₂ / \langle Si	3	0.15	1.85 ± 0.05	350-475
Al/Ti/SiO ₂ / \langle Si	this work	2.27	1.9 ± 0.1	460-515
Ti/Al/SiO ₂ / \langle Si	this work	3.64	2.0 ± 0.1	460-515
Ti/ \langle Al	this work	12.78	2.0 ± 0.1	460-515

rated bilayers on thin SiO₂ on Si wafers for the same evaporation conditions were simultaneously annealed in forming gas (nitrogen with 14.7% hydrogen), which was fed directly from a cylinder. Before sliding the boat with the samples in the isothermal zone of a tube furnace, the gas was kept flowing through the quartz tube for about 2 h at a temperature above that required for annealing.

Figures 5(a) and 5(b) show 1.8-MeV ⁴He⁺ back-

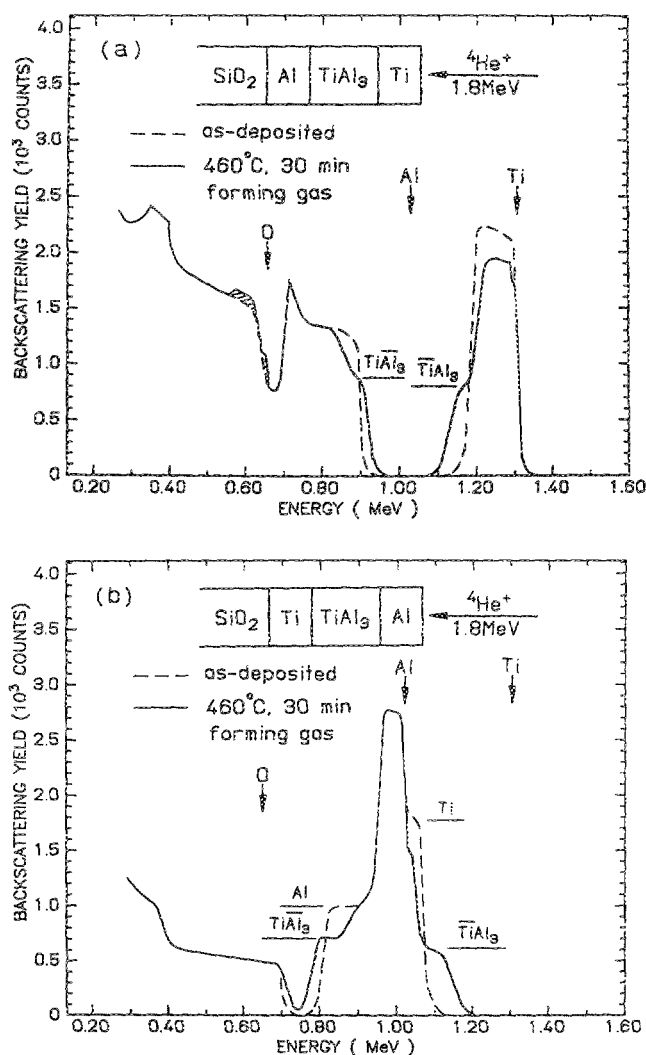


FIG. 5. 1.8-MeV ⁴He⁺ backscattering spectra for (a) Ti/Al/SiO₂, (b) Al/Ti/SiO₂, showing the effects of residual gas on the reaction of Ti/Al bilayer samples with bilayers of inversed sequence (annealing procedure 2).

scattering spectra for Ti/Al and Al/Ti couples before and after annealing at 460 °C for 30 min. As can be seen by comparing the widths of Ti signals in the compound, the reaction is more than two times faster when the Al is on top rather than Ti. An explanation is that bare Ti getters oxygen from the ambient during sintering. Evidence for that is found in the spectra of Fig. 5(a), where the signal height of unreacted Ti is obviously lower than that of as-deposited Ti. The flat top of the Ti signal after annealing indicates that oxygen is fairly uniformly distributed in the unreacted Ti film. The reduced height of the Ti signal upon annealing, or the ratio of the integrated oxygen and Ti signals near the surface for the annealed sample in Fig. 5(a), corresponds to an average oxygen concentration of about 30% in Ti. For the same heat treatment no oxygen signal is observed in either Ti or Al when Al is on top [Fig. 5(b)]. This condition is also verified by the fact that the highest peak near 1 MeV in the spectrum, which consists of overlapping Al and Ti signals, stays the same upon annealing. These comparisons clearly demonstrate that Al effectively prevents a major oxygen contamination of the Ti film. In other words, a sample with an Al film on top can indeed be considered a reference case for the present study in which oxygen from the surrounding ambients interferes little. That conclusion supports the assumption we made initially.

C. Annealing procedure 3 (vacuum, with protection)

A piece of pure Ti foil of 99.97% was used to wrap a sample of Ti/ \langle Al during annealing in order to minimize interference by residual gases in the vacuum. The Ti foil was cleaned with organic solvents and then baked out in a vacuum at 300 °C for a couple of hours prior to use. All samples considered in this section have been diced from one large piece, parts of which were used for the kinetics study of Sec. III A above. The annealing was performed in the same vacuum system at 450 °C, which is the temperature required to initiate reaction of Ti on a \langle Al substrate. The pretreatment of the annealing system was the same as for the annealing procedure 1.

The samples annealed for different durations were analyzed by 2-MeV ⁴He⁺ ion backscattering (see in Fig. 6). After 36 min of annealing, steps indicating the presence of a compound appear at the Ti/ \langle Al interface and the Ti surface. The steps are very clear after 81-min annealing, so that atomic composition ratios can be readily determined for both steps. The ratio of Ti to Al is about 1:3 for both. X-ray

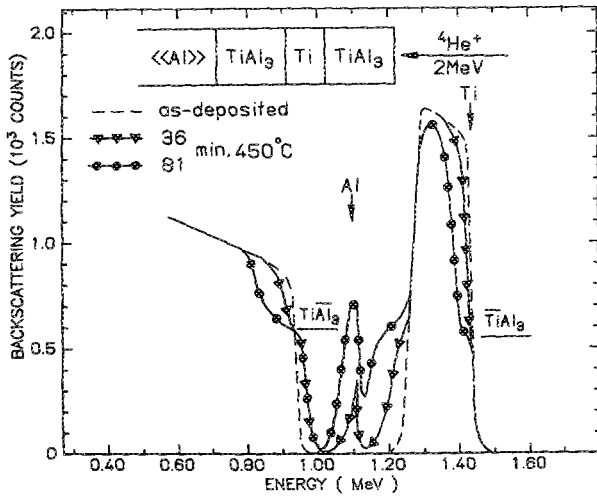


FIG. 6. 2-MeV $^4\text{He}^+$ backscattering spectra of Ti/Al samples wrapped by Ti foil during 450°C annealing for 36 min (triangles) and 81 min (circles). Al out-diffuses along grain boundaries to the free surface of Ti and forms TiAl_3 compound layer there, in addition to the interfacial layer described in Figs. 2(b), 3, and 4 (annealing procedure 3).

diffraction confirmed the presence of TiAl_3 . No other phase was detectable. The TiAl_3 layer formed at the interface is 2670 \AA thick. This is equal to that observed for a Ti/⟨Al⟩ sample annealed by procedure 1, assuming $K = 12.78 \text{ cm}^2/\text{s exp} - [2.0eV/kT]$ (see Table I). Thus, kinetics measured there are still valid for the present interfacial growth. Hence, the 1000-\AA layer at the surface constitutes an additional parallel process of TiAl_3 formation, for which Al, clearly, has to be the dominant moving species. An obvious interpretation is that the Al diffuses to the free surface along Ti grain boundaries.

This experiment has been executed with two independently prepared samples, over the whole annealing temperature range considered in this paper. The growth of TiAl_3 at both Ti film interfaces was always observed, although their thickness did vary a bit for equal annealing durations. We observed that the growth of a surface layer is particularly easy to reproduce when the Ti film is thick.

D. Impurity effects

The alert reader may have noticed that we have so far referred to oxygen whenever impurity effects were discussed, although the facts provided neither identify oxygen as the dominant impurity in terms of amounts, nor exclude a primary role by another element. It is indeed possible that elements other than oxygen are major players in the reactions described here. We shall nonetheless continue to ignore other impurities even though they are certainly present. Reasons are that oxygen is indeed present in our samples, is ubiquitous, and reacts strongly with both Al and Ti. Also, plausible interpretations of the observations can be given by invoking only oxygen. Finally, new conceptual insight is offered by the present data and their interpretation in terms of oxygen as a model case, because the influence of impurities, even those as common as a oxygen and carbon, is quite poorly documented so far for metal-metal thin-film reactions.

We measured the oxygen redistribution upon annealing of Ti/Al structures with the $^{16}\text{O}(\alpha,\alpha)^{16}\text{O}$ elastic resonant scattering technique. By varying the incident beam energy step by step, an oxygen profile was obtained for the following samples: (a) as-deposited, and annealed at 514°C for (b) 10 min, (c) 37 min, by procedure 1, and (d) after annealing at 450°C for 81 min by procedure 3 (Ti foil wrapping). A thermally oxidized Si wafer was used to calibrate the scattering yield. The resonance reaction method¹⁸ is about 30 times as sensitive to oxygen as normal backscattering spectra, but the depth resolution is poor. Although the FWHM of the surface resonance peak is 10 keV , the width widens as the peak penetrates the sample because of energy straggling. For instance, the FWHM is about 16 keV when the resonance peak is located at 1000 \AA of Ti or TiAl_3 , according to energy straggling in the two materials calculated from Bohr's theory.²³ The FWHM of the peak covers 470 \AA of Ti or 600 \AA of TiAl_3 . Consequently, this technique is unable to precisely profile interfacial oxygen distributions. The measured concentration values, however, are accurate to within 20 at. %.

Measured oxygen concentration (in atomic percent of the matrix) versus depth are plotted in Figs. 7 and 8 for the four cases described above. The as-deposited sample exposed to air for an extended duration [Fig. 7(a)] exhibits an ap-

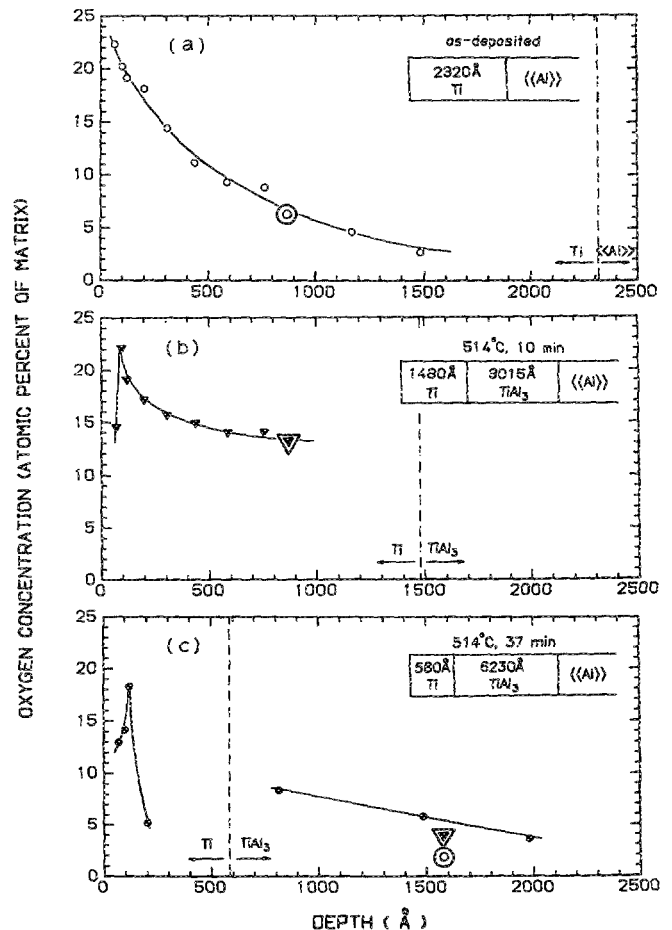


FIG. 7. Oxygen distributions obtained by $^{16}\text{O}(\alpha,\alpha)^{16}\text{O}$ elastic scattering resonance method for the following samples: (a) as-deposited and after annealing at 518°C for (b) 10 min, and (c) for 37 min following the annealing procedure 1.

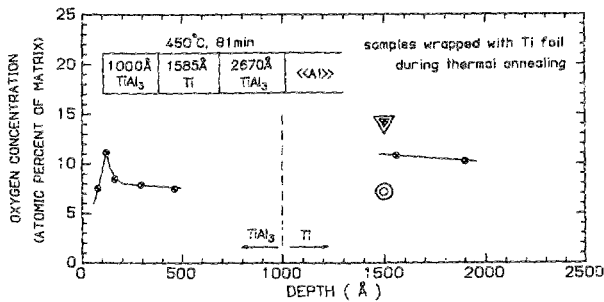


FIG. 8. As Fig. 7 except that the sample was wrapped with Ti foil during 450 °C annealing for 81 min according to annealing procedure 3. The double-lined symbols are those indicated in the same way in Figs. 7(a) and 7(b).

proximately exponential oxygen distribution with a thin $\text{TiO}_{0.25}$ surface layer. After 10 min annealing at 514 °C by procedure 1, one-third of the Ti film is transformed to TiAl_3 by reaction at the $\text{Ti}/\langle\text{Al}\rangle$ interface [Fig. 7(b)]. The oxygen in the unreacted Ti layer increases and is homogenized except for a narrow oxygen peak near the surface. The sample annealed for 37 min [Fig. 7(c)] has a thick aluminide layer. The oxygen distribution in it has a gradient similar to that observed in the unreacted Ti layer.

To understand the oxygen redistribution during reactions, it is helpful to note the change of oxygen concentration at a fixed depth. Consider, for example, an observation point in the 2320-Å-thick Ti lattice chosen 860 Å below the surface in the as-deposited Ti film [big open circle in Fig. 7(a)]. The transformation to TiAl_3 takes place by the motion of Al into the stationary Ti matrix. After a 37-min annealing at 514 °C, a Ti layer of 1740 Å is consumed and forms a TiAl_3 layer of 6230 Å. As shown in Fig. 7(c), the observation point shifts from 860 Å in the Ti film [Fig. 7(a)] to 1000 Å below the Ti/TiAl_3 interface, that is, 1580 Å below the surface. If the amount of oxygen measured in terms of a fraction of Ti atoms remains constant during the reaction, that same amount of oxygen measured in terms of a fraction of all matrix atoms after the reaction is reduced by a factor of 4 because each Ti atom has three added Al atoms. This calculation yields the two double-lined points at 1580 Å in Fig. 7(c) when starting from the corresponding points in Figs. 7(a) and 7(b) for the samples before and after a 10-min annealing, respectively. Clearly, the oxygen concentration at the observation point rises with annealing time as measured against the number of Ti atoms. The obvious interpretation of this outcome is that oxygen in the Ti is incorporated in the TiAl_3 compound. (We cannot ascertain that additional oxygen is picked up from the ambient, although this is probable, because the total amount of oxygen contained in the sample remains undetermined by the profiles given in the Figs. 7 and 8.) This incorporation of the oxygen during the reaction agrees with a model derived from studies of impurity effects in silicide reactions.¹⁴ The model says that an impurity will be incorporated in a growing compound when the impurity is located in the stationary species and is immobile there. The model does not strictly apply here since some redistribution of oxygen is in fact observed [Figs. 7(a) and 7(b)].

Incorporation can also be seen in the wrapped sample

after 450 °C annealing (see Fig. 8). The oxygen distribution in the TiAl_3 layer near the surface is similar to that seen in the unreacted Ti portion of the annealed sample shown in Figs. 7(b) or 7(c), except for concentration. It is worth mentioning that the oxygen peak of the TiAl_3 surface layer in Fig. 8 should have occurred near 360 Å if it had been immobile with respect to Ti [corresponding to the 100 Å of Ti in Figs. 7(b) and 7(c)]. In fact, the peak shifts toward the surface with respect to the Ti lattice and the concentration rises, which may mean that oxygen is mobile and dissolved in TiAl_3 . The two points (⊙, ▽) at 1580 Å of Fig. 8 are again deduced from the same data points used before in Figs. 7(a) and 7(b) by assuming that oxygen is immobile in Ti.

IV. DISCUSSION

A. Transport through TiAl_3

We find in agreement with others^{3,4} that upon thermal annealing the TiAl_3 compound forms at Ti/Al interface, and that the kinetics are diffusion controlled. The activation energy is independent of the sequence of the metal layers and is the same for large-grained and evaporated Al. The sample with Ti on top is more subject to oxygen contamination [Figs. 5(a), 7, and 8] than the sample with Al on top [Fig. 5(b)]. The oxygen contained in Ti and TiAl_3 can exceed 10 at. % in our cases. In contrast, only 0.25-at. % Cu in the Al raises the activation energy of TiAl_3 formation by 25%.⁹ Tardy and Tu suggest that the moving species (Al) transverse the TiAl_3 layer by lattice diffusion via Al vacancies. They explain the role of Cu on the basis that Cu atoms occupy Al sites in TiAl_3 compound and in this way alter the diffusion mechanism of Ti. Although the contribution of Ti to the mass flow is only on the order of 0.1,^{9,14} it is its reduction that decreases the reaction constant by about a factor of 2 and raises the activation energy. In contrast, we find the same activation energy in all our experiments, even though the amount of oxygen contained in the compound varies (Figs. 7 and 8). This argues for an interstitial position of oxygen. Whatever the position of the oxygen in TiAl_3 actually is, the results indicate that the transport of Al through TiAl_3 decreases when the oxygen concentration rises, but always without altering the diffusion mechanism significantly.

These ideas ignore the role of grain-boundary diffusion through the compound layer. Krafcsik *et al.* consider that Al diffusion along grain boundaries of TiAl_3 can be an important mechanism, and Wittmer, Goues, and Huang⁸ support this contention by associating large TiAl_3 with small reaction constants. If grain-boundary diffusion of Al is important in the compound, the purest sample would be expected to have the lowest activation energy for the reaction constant. Figure 4 is consistent with this idea, because the two most recent contributions (Tardy *et al.* and Wittmer *et al.*) report the lowest activation energy (1.7 and 1.6 eV), and the oxygen concentration is measured to be 1 at. % or less in their as-deposited films. Other experimentors have unspecified oxygen concentration, and activation energies for the reaction constant that are near 2.0 eV. Our experiments provide no information on the diffusion mechanism through the

aluminide film. Since we measure an oxygen concentration on the order of 10 at. % in the compound, it is possible that Al diffuses mainly through the TiAl_3 grains, hence our high activation energy.

B. Nucleation and growth of the surface compound layer

A new insight in the transport of Al through Ti is provided here by the experiment described in Sec. III C and summarized by the results of Fig. 6. In this sample TiAl_3 forms simultaneously at the $\text{Ti}/\langle\langle\text{Al}\rangle\rangle$ interface and the vacuum/Ti interface. To form such a surface layer of TiAl_3 , there must be a flux of Al through the Ti. Two questions arise: (i) why has this effect not been observed previously, and (ii) what causes it to occur?

Before addressing the questions raised by this experiment, we recall that all previous studies of the Ti/Al interaction have made use of the sample configuration with Al on top, Ti below, and a SiO_2 substrate. A TiAl_3 layer was never seen to form at the SiO_2/Ti interface. That is so even in the most recent studies where presumably the oxygen concentration is low. In one case, the Al content in the unreacted Ti after annealing is reported to be about 4 at. % and rather uniformly distributed over the Ti film.⁹ Therefore, it is evident that in such experiments the transport of Al is possible. This conclusion is in accord with the diffusivity of Al in Ti [$D = 9.58 \times 10^{-5} \text{ cm}^2/\text{s} \exp(-1.19\text{eV}/kT)$ in the temperature range 700–850 °C].²⁴ An extrapolation to 450 °C predicts that it takes only 5 min to traverse 2500 Å of Ti. This agreement is perhaps misleading because the diffusion constant reported in the literature varies very much,^{25,26} and we prefer the experimental argument cited first. In short, it must be the absence of nucleation that prevents the growth of TiAl_3 in that configuration, not the lack of transport. These arguments lead to the conclusion that nucleation is facile at an open Ti surface as realized in the experiment of Fig. 6, but difficult at a Ti interface with SiO_2 . Such a difference is acceptable. From the ideas of classical nucleation theory, it is the surface tension that determines the activation energy of nucleation. The surface tension at the Ti/SiO_2 interface and at an open Ti surface are likely to be different.

In accordance with these ideas, we find that the open Ti surface of our samples annealed without a Ti wrapping foil does not exhibit nucleation. (Our facts do not actually eliminate Al transport as the main obstacle, but the preceding discussion convincingly does.) The presence of the wrapping foil evidently alters the state of the Ti surface during annealing. We believe that it is the reduction of the oxygen in the surface layer of the Ti film of the sample that promotes nucleation. It is known that Ti can form surface layers when oxygen is present in the range of partial pressures likely to exist in our annealing furnace.²⁷ This surface layer rapidly dissolves in the bulk of the Ti when the temperature rises. The competition between growth and dissolution of the surface oxide layer is quite abrupt and falls in the range of 400–500 °C. This is precisely the range typically encountered in our heat treatments. Transient effects must thus be expected to play a role here, in addition to the initial content of oxygen

in the sample and the residual oxygen in the annealing ambient. In other words, these experiments are critically dependent on details, and their reproducibility is correspondingly difficult to assure.

One can reduce all of the observations reported here to the following set of assumptions:

- (i) Excessive oxygen in the surface layer of the Ti suppresses nucleation of TiAl_3 ;
- (ii) SiO_2 in contact with the Ti film inhibits nucleation of TiAl_3 ;
- (iii) TiAl_3 does not nucleate homogeneously in Ti; and
- (iv) Al can always diffuse readily through the Ti film.

As deposited, the Ti film has a significant oxygen concentration at the surface. When the Ti films are exposed to the ambient during annealing and without a Ti wrapping foil, oxygen penetrates into the bulk of the Ti film by breakdown of the surface oxide layer and by additional pickup from the ambient. The bulk oxygen concentration increases as a result [Fig. 7(b)]. The compound layer that grows below is a sink for oxygen. The oxygen concentration thus decreases just below the surface layer when the growing compound comes near it [Fig. 7(c)]. No compounds nucleate at the surface because the oxygen concentration there remains too high. This scenario is altered in the presence of the clean Ti wrapping foil. The foil reduces the partial pressure of oxygen near the sample surface and accelerates the breakdown of the surface layer of oxide on the Ti film.²⁷ That this effect is present follows also from Fig. 8. Nucleation now sets in at the surface as well as at the interface with the Al.

When the Ti wrapping foil reduces the oxygen in the surface layer of the Ti film, the oxygen concentration within the bulk of the Ti film decreases as well. Conversely, without the wrapping foil, the oxygen concentration will be high in the bulk and the surface layer of the Ti film simultaneously. In that case, the absence of a surface layer growth may thus also be the result of a diminished Al transport. The present experiment cannot distinguish between these two causes.

C. Polycrystalline Al film versus $\langle\langle\text{Al}\rangle\rangle$

The picture drawn thus far is complicated by an additional observation that will now be described, but that cannot be explained on the basis of the stated assumptions. When a polycrystalline evaporated Al film on SiO_2 is substituted for the large-grained $\langle\langle\text{Al}\rangle\rangle$ substrate, a surface compound layer will not form, even when the annealing is done with a protecting Ti wrapping foil and when simultaneously, in the same boat of the vacuum annealing furnace, a large-grained $\langle\langle\text{Al}\rangle\rangle$ sample is included that will show the compound formation on the sample surface. This experiment was performed twice with independently evaporated Ti/Al films and no difference in the outcome. The two samples in this experiment differed only in two ways: the source of Al (large-grained $\langle\langle\text{Al}\rangle\rangle$ versus evaporated thin polycrystalline Al film of 3410 Å on SiO_2), and the thickness of evaporated Ti layer (2320-Å Ti on $\langle\langle\text{Al}\rangle\rangle$ versus 1800-Å Ti on polycrystalline Al). Further experiments will be required to clarify this observation.

V. SUMMARY AND CONCLUSION

We have investigated the interfacial interactions that occur in Al/Ti/SiO₂, Ti/Al/SiO₂, and Ti/⟨Al⟩ samples annealed in the temperature range 450–515 °C. It has been found that the growth of TiAl₃ at the Al/Ti interface is a diffusion-limited process characterized by an activation energy of 1.9–2.0 eV for all three cases, but the rate of growth is not the same, i.e., the pre-exponential factors (listed in Table I) differ. We believe that the Al transport mechanism is independent of the oxygen contamination for the concentration levels (15 at. %) considered here.

The residual gas contents in the as-deposited Ti film and in the annealing ambient have a pronounced effect on aluminide growth rate. The growth constant for a sample with the Ti bilayer on the top is half of that for a sample with the Al film on top. A thin surface oxide of Ti forms rapidly when an as-deposited film is exposed to air and the ambient during a subsequent thermal annealing. The oxygen also redistributes in the Ti during annealing. Oxygen present in the Ti is incorporated in the TiAl₃ compound during its formation even though oxygen is mobile in Ti film.

The use of a clean Ti wrapping foil reduces the residual oxygen partial pressure near the surface of the sample. The surface oxide layer formed when the as-deposited Ti is exposed to air can dissociate during heat treatment. The foil keeps the oxygen concentration in the bulk of the Ti film lower than that in the unwrapped sample. As a result, nucleation at the free Ti surface occurs, which results in the formation of the aluminide at the surface of the Ti/⟨Al⟩ sample.

By backscattering spectra, there is no noticeable difference in the sharpness of the edges of the compound layers that grows at Ti/Al interface, regardless of the sample configuration and the oxygen content.

ACKNOWLEDGMENTS

We are grateful to R. Gorris for technical assistance and to Dr. A. J. Brunner for helpful discussions. This work was

financially supported in part by the Office of Naval Research under Contract No. N00014-84-K-0275.

- ¹C. Y. Ting and M. Wittmer, *Thin Solid Films* **96**, 327 (1982).
- ²C. Y. Ting and B. L. Crowder, *J. Electrochem. Soc.* **129**, 2590, (1982).
- ³R. W. Bower, *Appl. Phys. Lett.* **23**, 99 (1973); and Ph.D. thesis (California Institute of Technology, Pasadena, CA, 1973).
- ⁴J. K. Howard, R. F. Lever, and P. J. Smith, *J. Vac. Sci. Technol.* **13**, 68 (1976).
- ⁵K. Nakamura, S. S. Lau, M.-A. Nicolet, and J. W. Mayer, *Appl. Phys. Lett.* **28**, 277 (1976).
- ⁶I. Krafcsik, J. Gyulai, C. J. Palmstrom, and J. W. Mayer, *Appl. Phys. Lett.* **43**, 1015 (1983).
- ⁷H.-C. W. Huang and M. Wittmer, *Mater. Res. Soc. Symp. Proc.* **25**, 157 (1984).
- ⁸M. Wittmer, F. Le Goues, and H.-C. W. Huang, *J. Electrochem. Soc.* **132**, 1450 (1985).
- ⁹J. Tardy and K. N. Tu, *Phys. Rev. B* **32**, 2070 (1985).
- ¹⁰R. K. Ball and A. G. Todd, *Thin Solid Films* **149**, 269 (1987).
- ¹¹R. K. Mahar and N. M. Devashrayee, *Appl. Phys. Lett.* **50**, 19 (1987).
- ¹²E. G. Colgan and J. W. Mayer, *Nucl. Instrum. Methods B* **17**, 242 (1986).
- ¹³X.-A. Zhao, H.-Y. Yang, E. Ma, and M.-A. Nicolet, *J. Appl. Phys.* **62**, 1821 (1987).
- ¹⁴C.-D. Lien and M.-A. Nicolet, *J. Vac. Sci. Technol. B* **2**, 738 (1984), and references therein.
- ¹⁵M. A. Harith, J. P. Zhang, S. U. Campisano, and H.-J. Klaar, *Appl. Phys. A* **42**, 35 (1987).
- ¹⁶R. Konishi, H. Sasaki, and S. Kato, *Jpn. J. Appl. Phys.* **22**, 1659 (1983).
- ¹⁷G. Ottaviani, F. Nava, G. Queirolo, G. Iannuzzi, G. De Santi, and K. N. Tu, *Thin Solid Films* **146**, 201 (1987).
- ¹⁸X.-A. Zhao, T. C. Banwell, and M.-A. Nicolet, *SPIE* **623**, 255 (1986).
- ¹⁹R. E. Smallman, in *Modern Physical Metallurgy*, 4th ed. (Butterworths, London, 1985), Chap. 10.
- ²⁰W.-K. Chu, J. W. Mayer, and M.-A. Nicolet, *Backscattering Spectrometry* (Academic, New York, 1978).
- ²¹X.-A. Zhao, E. Ma, H.-Y. Yang, and M.-A. Nicolet, *Thin Solid Films* (in press).
- ²²W. B. Pearson, *A Handbook of Lattice Spacing and Structures of Metals and Alloys* (Pergamon, Oxford, 1967), Vol. 2.
- ²³N. Bohr, *K. Dan. Vidensk. Selsk. Mat.-Fys. Meed.* **18**, 8 (1948).
- ²⁴A. V. Pokoev, V. M. Mironov, and L. K. Kudryavtseva, *Sov. J. Non-Ferrous Met.* **2**, 81 (1976).
- ²⁵J. Raisanen, A. Anittila, and J. Kenonen, *J. Appl. Phys.* **57**, 613 (1985).
- ²⁶V. B. Rao and C. R. Houska, *Metall. Trans.* **14A**, 61 (1983).
- ²⁷T. Smith, *Surf. Sci.* **38**, 292 (1973).